The ISME Journal (2017) 11, 1651–1666

www.nature.com/ismej

ORIGINAL ARTICLE

Integrated metabolism in sponge–microbe symbiosis revealed by genome-centered metatranscriptomics

Lucas Moitinho-Silva[1], Cristina Díez-Vives[1], Giampiero Batani[1], Ana IS Esteves[1], Martin T Jahn[2] and Torsten Thomas[1]

[1]*Centre for Marine Bio-Innovation and School of Biological, Earth and Environmental Sciences, The University of New South Wales, Sydney, New South Wales, Australia and* [2]*Marine Microbiology, GEOMAR Helmholtz Centre for Ocean Research, Kiel, Germany*

Despite an increased understanding of functions in sponge microbiomes, the interactions among the symbionts and between symbionts and host are not well characterized. Here we reconstructed the metabolic interactions within the sponge *Cymbastela concentrica* microbiome in the context of functional features of symbiotic diatoms and the host. Three genome bins (CcPhy, CcNi and CcThau) were recovered from metagenomic data of *C. concentrica*, belonging to the proteobacterial family *Phyllobacteriaceae*, the *Nitrospira* genus and the thaumarchaeal order *Nitrosopumilales*. Gene expression was estimated by mapping *C. concentrica* metatranscriptomic reads. Our analyses indicated that CcPhy is heterotrophic, while CcNi and CcThau are chemolithoautotrophs. CcPhy expressed many transporters for the acquisition of dissolved organic compounds, likely available through the sponge's filtration activity and symbiotic carbon fixation. Coupled nitrification by CcThau and CcNi was reconstructed, supported by the observed close proximity of the cells in fluorescence *in situ* hybridization. CcPhy facultative anaerobic respiration and assimilation by diatoms may consume the resulting nitrate. Transcriptional analysis of diatom and sponge functions indicated that these organisms are likely sources of organic compounds, for example, creatine/creatinine and dissolved organic carbon, for other members of the symbiosis. Our results suggest that organic nitrogen compounds, for example, creatine, creatinine, urea and cyanate, fuel the nitrogen cycle within the sponge. This study provides an unprecedented view of the metabolic interactions within sponge–microbe symbiosis, bridging the gap between cell- and community-level knowledge.
The ISME Journal (2017) **11,** 1651–1666; doi:10.1038/ismej.2017.25; published online 24 March 2017

Introduction

A wide range of animals are found in symbiosis with microorganisms, from basal metazoans, such as marine sponges (phylum *Porifera*), to humans (phylum *Chordata*) (Taylor *et al.*, 2007; Cho and Blaser, 2012). Animal–microbe symbioses encompass a variety of acquisition modes (that is, vertical, horizontal and a combination of both; for example, Cary and Giovannoni (1993); Kikuchi *et al.* (2007); Schmitt *et al.* (2008)), and levels of diversity (ranging from monoclonal populations to highly complex assemblages; Martens *et al.* (2003); Schmitt *et al.* (2012)). Additionally, a gradient of interactions may occur, ranging from competition to mutualism (Dethlefsen *et al.*, 2007; Coyte *et al.*, 2015; Thomas *et al.*, 2016). To account for this spectrum of patterns, Douglas and Werren (2016) have recently argued that host–microbe symbioses are productively approached as ecological communities. Therefore, to further our understanding of the biology of animal–microbe symbioses, research should contemplate the members of the association, that is, the microbial populations and the host, and how they relate to each other.

Marine sponges are filter-feeders found in a wide range of benthic environments, across gradients of depth and latitude (Wulff, 2012). Sponges perform a broad range of functional roles in benthic habitats (Bell, 2008), including the retention of nutrients and energy within the coral reef through the consumption of dissolved organic matter (DOM) and high cell turnover rates (Yahel *et al.*, 2003; de Goeij *et al.*, 2013). In addition to DOM, sponges feed on detritus and microorganisms of diverse sizes (from 0.5 to 70 μm) (Marta *et al.*, 1999; Hadas *et al.*, 2009). Owing to their basal position in metazoans phylogeny and their association with microbial communities, sponges are emerging as models for the evolutionary study of animal–microbe symbiosis (for example, Fan *et al.*, 2012; Ryu *et al.*, 2016).

Microbial communities can account for up to 40% of the sponge tissue volume and often contain novel and uncharacterized diversity (Taylor *et al.*, 2007; Schmitt *et al.*, 2012). Microorganisms are generally

Correspondence: T Thomas, Centre of Marine Bio-Innovation and School of Biological, Earth and Environmental Sciences, The University of New South Wales, High Street, Sydney, New South Wales 2052, Australia.
E-mail: t.thomas@unsw.edu.au
Received 3 October 2016; revised 10 January 2017; accepted 19 January 2017; published online 24 March 2017

found in the animal's extracellular matrix (mesohyl), although they are not restricted to this location (Taylor *et al.*, 2007). Owing to the lack of culturable representatives of the microbiome, most of the understanding of the functional roles of microbial symbiont have been acquired by approaches either centered on the community, for example, using meta-omics, 16S rRNA gene analysis and compound-uptake experiments, or on specific genomes, pathways and genes (reviewed by Taylor *et al.*, 2007 and Webster and Thomas 2016). Together, these studies have revealed important metabolic attributes of sponge-associated microorganisms, such as different energy acquisition strategies (for example, heterotrophism and autotrophism), complex element cycling, functional equivalence, production of bioactive compounds and nutrient transfer to the host (Hoffmann *et al.*, 2009; Fan *et al.*, 2012; Freeman *et al.*, 2013; Kamke *et al.*, 2013; Wilson *et al.*, 2014). Nevertheless, the metabolic interactions among the microbiome members and between them and the host cells are rarely explored and thus remain largely unknown (Webster and Thomas, 2016).

The sponge *Cymbastela concentrica* contains consistently dominant and uncharacterized alphaproteobacterial symbionts, particularly within the family *Phyllobacteriaceae* (Taylor *et al.*, 2004; Fan *et al.*, 2012; Esteves *et al.*, 2016) as well as community members belonging to the *Gammaproteobacteria*, the *Nitrospira* and the archaeal phylum *Thaumarchaeota* among others (Fan *et al.*, 2012; Esteves *et al.*, 2016). In addition, *C. concentrica* hosts an abundant population of diatoms (Taylor, 2005). The overall community composition and function of the *C. concentrica* microbiome have been previously characterized on the community level using metagenomics, metaproteomics and metatranscriptomics (Díez-Vives *et al.*, 2016; Thomas *et al.*, 2010; Liu *et al.*, 2011; Fan *et al.*, 2012; Liu *et al.*, 2012). Here we build on these data sets to unveil nutritional interactions in *C. concentrica*. Towards this goal, we reconstructed three new prokaryotic genomes and estimated their activity by analyzing metatranscriptomic sequences, while metabolic features of the sponge and diatoms were inferred from an eukaryotic transcriptomic data set produced from *C. concentrica*.

Materials and methods

Genome assembly, binning and annotation

Metagenomic shotgun sequencing reads for three replicates (BBAY40, 41 and 42) of the microbiome of *C. concentrica* from a previous study (Fan *et al.*, 2012) were co-assembled using the Newbler assembler (Roche, Penzberg, Germany). Sequence reads for each replicate were then mapped back against assembled contigs >500 bp using the Bowtie aligner (Langmead *et al.*, 2009). Coverage file and contigs were then used to bin and refine genomes using the GroopM tool (Imelfort *et al.*, 2014). Genome bins were checked for completeness and contamination using CheckM (Parks *et al.*, 2015) and then annotated using the IMG system (Markowitz *et al.*, 2014). Genome assembly and annotation are avaiable at IMG (http://img.jgi.doe.gov) under the genome IDs 2608642157, 2608642160 and 2626541593. Phylogenetic analysis of 16S rRNA genes and deduced amino-acid sequences for those bins are described in Supplementary Information.

Transcriptomic analysis

We used the metatranscriptomic reads from the microbiome of three *C. concentrica* individuals (Díez-Vives *et al.*, 2016) to estimate the gene expression of binned genomes. Briefly, mRNA was previously enriched from three individuals (ind1, ind2, and ind3; biological replicates), which were processed with Dynabeads Oligo $(dT)_{25}$ (Thermo Fisher Scientific, Waltham, MA, USA) and the Ribo-Zero Bacteria Kit (Epicentre, Madison, WI, USA) in technical replicates (aR and bR). Enriched prokaryotic mRNA was sequenced with HiSeq2000 platform (Illumina, San Diego, CA, USA) with 100 bp paired-end reads. Transcript expression for the coding DNA sequences (CDS) of each genome bin was estimated with RSEM v. 1.2.21 (Li and Dewey, 2011) with default parameters, which implements the Bowtie aligner (Langmead *et al.*, 2009). Transcripts per million (TPM) measures were used as estimations of expression (Li *et al.*, 2010; Wagner *et al.*, 2012). Gene expression estimates in each sponge individual were obtained by averaging TPM values of the technical replicates. Only genes with mapped reads (replicate-average $TPM>0$) coming from at least two of the three sponge individuals were considered expressed. The global expression estimate for each gene was obtained by averaging TPM values (TPM_{av}) across the three sponge individuals.

The analysis of eukaryotic transcripts is described in Supplementary Information. Briefly, transcripts were taxonomically sorted using the Lowest Common Ancestor algorithm implemented in MEGAN v. 5.11.3 (Huson *et al.*, 2011). Peptides deduced from predicted coding sequences were annotated based on the Kyoto Encyclopedia of Genes and Genomes (KEGG) Orthology (KO). Expression estimates of KEGG functions were calculated by summing TPM values (TPM_{sum}) across coding sequences.

Localization analysis of symbionts

Three individuals of *C. concentrica* were collected by SCUBA diving from Botany Bay near Bare Island, Sydney, Australia (33.99222° S, 151.23111° E) during October 2015. Specimens were processed, fixed and dehydrated. Probes specific for the obtained genome bins (that is, CcPhy, CcNi and CcThau; see

Table 1 Assembly and annotation statistics of genome bins

	CcPhy (Ga0068441)	*CcNi (Ga0068443)*	*CcThau (Ga0078905)*
Assembly size (bp)	2 116 962	1 594 656	2 161 854
Individual coverage in three replicate metagenomes	19.5 × /58.4 × /37.5 ×	3.2 × /0.8 × /7.2 ×	0.9 × /15.2 × /2.3 ×
Estimated genome completeness (%)	69.17	66.56	97.12
Estimated contamination (%)	0.39	0	4.01
Number of contigs	918	126	637
Average GC content (%)	60.34	48.03	38.42
Number of CDS	2411	1679	2745
Number of rRNA genes	1	3	5
Number of tRNA genes	16	25	44

Abbreviations: CDS, coding DNA sequence; GC, guanine–cytosine; rRNA, ribosomal RNA; tRNA, transfer RNA.

below) were designed and cells were detected using fluorescence *in situ* hybridization. Sample processing, probe design and fluorescence *in situ* hybridization conditions are fully described in Supplementary Information.

Results and discussion

Genomes and transcriptomes of the dominant community members in C. concentrica

Three genomes were reconstructed (Table 1) from a previous metagenomic sequence data set of the microbial community of *C. concentrica* (Fan *et al.*, 2012). Phylogenetic analysis of the 16S rRNA gene sequence recovered from one of the genomes (Ga0068441) placed it with members of the family *Phyllobacteriaceae*, order *Rhizobiales*, class *Alphaproteobacteria* (Supplementary Information; Supplementary Figure S1). Thus the genome will be hereafter referred to as CcPhy (*C. concentrica Phyllobacteriaceae*). The 16S rRNA gene sequence is only 96% similar to its closest cultured bacterium (*Mesorhizobium amorphae* CCNWGS0123) and has >99% similarity to sequences that have been previously found in *C. concentrica* (for example, GenBank: AY942778.1). The cluster represented by these *C. concentrica*-derived sequences represents a distinct and novel clade within the *Phyllobacteriaceae* (Supplementary Figure S1). The 16S rRNA gene sequence of the second genome (Ga0068443) was phylogenetically close to other sequences derived from several sponge species (for example, *Agelas dilatata*, *Geodia barretti*, *Xestospongia testudinaria*). These sequences were related yet distinct from sequences of the lineage IV of the *Nitrospira* genus within the phylum *Nitrospirae* (Supplementary Information; Supplementary Figure S2). The genome will be hereafter named CcNi. The 16S rRNA gene sequence of the last genome obtained (Ga0078905) clustered within the candidate order *Nitrosopumilales* (known as group I.1a) (Konneke *et al.*, 2005; Stieglmeier *et al.*, 2014b) within the *Thaumarchaeota* phylum (Supplementary Information; Supplementary Figure S3). It will be referred as CcThau. The 16S rRNA sequence from CcThau was 99% similar to the sequence from *Candidatus* Nitrosopumilus sediminis AR2 (GenBank: CP003843.1). According to studies based on OTUs recovered from metagenomic data sets and 16S rRNA gene sequencing, these three organisms are among the most dominant members of the *C. concentrica* microbiome (Thomas *et al.*, 2010; Fan *et al.*, 2012; Esteves *et al.*, 2016). For example, based on 16S rRNA gene sequencing, the *Phyllobacteriaceae* OTU may account approximately 17% of all bacteria in the sponge, while the *Nitrospira* OTU has a relative abundance of ~6% (Thomas *et al.*, 2010). Metagenomic sequencing further indicated that the thaumarchaeal organism has similar relative abundances than the *Nitrospira* bacterium (Fan *et al.*, 2012).

CcThau has the largest genome assembly with a size of 2.16 mega basepairs (Mb), followed by CcPhy with 2.11 Mb and CcNi with 1.59 Mb (Table 1). Genome completeness estimations based on lineage-specific marker genes were higher in CcThau (97.12%) in comparison to CcPhy (69.17%) and CcNi (66.56%). The estimated contamination of genome bins was low, ranging from 0% to 4.01%. GC content varied from 38.42% for CcThau and 48.03% for CcNi to 60.34% for CcPhy. Metatranscriptomic sequencing reads mapped to these genomes at different extent, where most of the reads mapped to the CcThau CDS (88 303 ± 23 580; mean ± s.d.), followed by CcPhy (16 540 ± 6128) and CcNi (7054 ± 3542) (Supplementary Table S1). Expressed genes represented 86.7% of the total CDS in CcPhy (2092 of 2411), 80.5% in CcNi (1353 of 1679) and 64.6% in CcThau (1775 of 2745). High gene expression correlation among biological replicates, as estimated by TPM values, indicated low variability between sponge individuals (Supplementary Information; Supplementary Figures S4). Average TPM values (TPM_{av}) of expressed genes across sponge individuals varied from 1.09 to 27 022.43, with a median of 191.54 in CcPhy, 354.2 in CcNi and 49.18 in CcThau (Supplementary Figure S7).

A heterotrophic, facultative anaerobic metabolism of CcPhy

The genomic and transcriptomic data suggest that the population represented by CcPhy has a

heterotrophic metabolism, which is broadly consistent with other members of the family *Phyllobacteriaceae* (Willems, 2014). The CcPhy expressed an almost complete set of genes for glycolysis (Embden–Meyerhof–Parnas pathway) (TPM_{av} 24–343; lower value – higher value), as well as the anabolic enzyme fructose-1,6-bisphosphatase (TPM_{av} 281 ± 39; mean ± s.d.) and tricarboxylic acid (TCA) pathways (TPM_{av} 121–1396), which are linked by the pyruvate dehydrogenase complex (TPM_{av} 88–1316) (Figure 1; Supplementary Table S2). Additionally, CcPhy is able to process sugars via the pentose phosphate pathway. In support of a heterotrophic lifestyle, approximately 13.5% of the protein-coding genes ($n = 328$) were involved in membrane transport (according to Transporter Classification Database (TCDB); Supplementary Table S2). From these, 164 CDS were assigned to the adenosine triphosphate (ATP)-binding cassette (ABC) superfamily (TC: 3. A.1), which were among the most expressed genes in the CcPhy transcriptome (Figure 2). The most expressed genes classified by TCDB encoded for components of different transport systems involved in the uptake of general L-amino acids, glycine betaine/proline, multiple sugars, spermidine/putrescine, monosaccharides, mannitol/chloroaromatic compounds, amino acid/amide and manose/fructose/ribose. Genes encoding for Amt-type ammonium transporters (TPM_{av} 1729 ± 351) and the glutamine synthase-glutamine oxoglutarate aminotransferase pathway (TPM_{av} 168–1157) were expressed, allowing for import and assimilation of extracellular ammonium (Javelle *et al.*, 2005).

Genes for the malate synthase and isocitrate lyase (TPM_{av} 211–605) were also expressed. These two enzymes are key for the glyoxylate cycle and their expression is an indication of aerobic growth on fatty acids and acetate (White, 2007). Active uptake of fatty acids could be carried by the product of expressed genes encoding for the proposed fatty acid transporter family (TPM_{av} 80–790). Several genes, whose products are involved in the fatty acid β-oxidation pathway and the downstream propanoyl-CoA degradation pathway were also found expressed (TPM_{av} 88–790) (Supplementary Table S2). Despite existing characterization of the fatty acid contents in sponges and associated bacteria (Gillan *et al.*, 1988; Koopmans *et al.*, 2015), this is to our knowledge the first report of heterotrophic fatty acid-based metabolism of bacteria associated with sponges. Future research focusing on the importance of fatty acids as energy source for sponge microbiome members and the origin of these compounds has the potential to elucidate the ecological relevance of this metabolic feature.

Creatinine degradation via creatine is used by bacteria to assimilate carbon and/or nitrogen (Kim *et al.*, 1986; Shimizu *et al.*, 1986). CcPhy expressed genes related to the degradation of creatine to glycine, that is, creatinase (TPM_{av} 151 ± 25) and the sarcosine oxidase alpha, beta, gamma and delta subunits (TPM_{av} 122–296). A gene encoding for creatinine amidohydrolase was present in the genome but not expressed. Urea is a product of this pathway, which is generated by the hydrolysis of creatine by creatinase (Shimizu *et al.*, 1986). The genome bin CcPhy lacked genes encoding for enzymes involved in the breakdown of urea into ammonium and inorganic carbon (Solomon *et al.*, 2010). Because the genome is not complete and the fact that urease activity has been described in the species of the *Phyllobacteriaceae* family (for example, Peix *et al.*, 2005), the existence and expression of *Phyllobacteriaceae*-like urease genes was further investigated for the *C. concentrica* microbiome. We found transcripts encoding for sequences similar to urease subunits and accessory proteins in the metatranscriptome of *C. concentrica* (Díez-Vives *et al.*, 2016), but none were related to sequences from *Phyllobacteriaceae* (Supplementary Information; Supplementary Table S3), further corroborating the absence of urea breakdown in CcPhy.

Members of the *Phyllobacteriaceae* family are described as having respiratory metabolism with oxygen as the terminal electron acceptor, while anaerobic nitrate respiration and facultative chemolithotrophic metabolism also exist for some members of the family (Willems, 2014). CcPhy has the genetic repertoire to thrive in a variety of oxygenic conditions. The genome encodes for the subunits of two different heme–copper terminal oxidases, the mitochondrial-like aa3-type cytochrome *c* oxidase and the cbb3-type cytochrome *c* oxidase. Both these oligomeric cytochrome complexes transfer electrons of the respiratory chain to its final destination, oxygen, but have different O_2 affinities and can be differentially regulated according to available oxygen concentrations (Garcia-Horsman *et al.*, 1994; Morris and Schmidt, 2013). For instance, in *Bradyrhizobium japonicum* (family *Bradyrhizobiaceae*) the low affinity aa3-type is favored in fully aerobic conditions, while the high affinity cbb3-type is used in microaerobic conditions (Gabel and Maier, 1993; Preisig *et al.*, 1996; Swem *et al.*, 2001).

Genomic data also indicated that, in the absence of O_2, CcPhy can perform nitrate (NO_3^-) respiration, where the membrane-bound nitrate reductase NarGHI complex transfers the electrons to nitrate, reducing it to nitrite (NO_2^-; Bertero *et al.*, 2003). In this case, it is likely that nitrite is excreted via a nitrate/nitrite transporter NarK as the final product of the CcPhy anaerobic respiration. Nitrite excretion is likely because the genome lacked genes encoding for enzymes capable to further reduce nitrite to nitric oxide (NO), that is, a copper or a cytochrome cd1-containing nitrite reductase (NirK and NirS, respectively), or to ammonium (NH_4^+), that is, cytochrome *c* nitrite reductase (NrfA) (Kraft *et al.*, 2011; Zheng *et al.*, 2013). The components and related genes of the cytochrome *c* oxidases and respiratory nitrate reductase were all expressed and also at similar

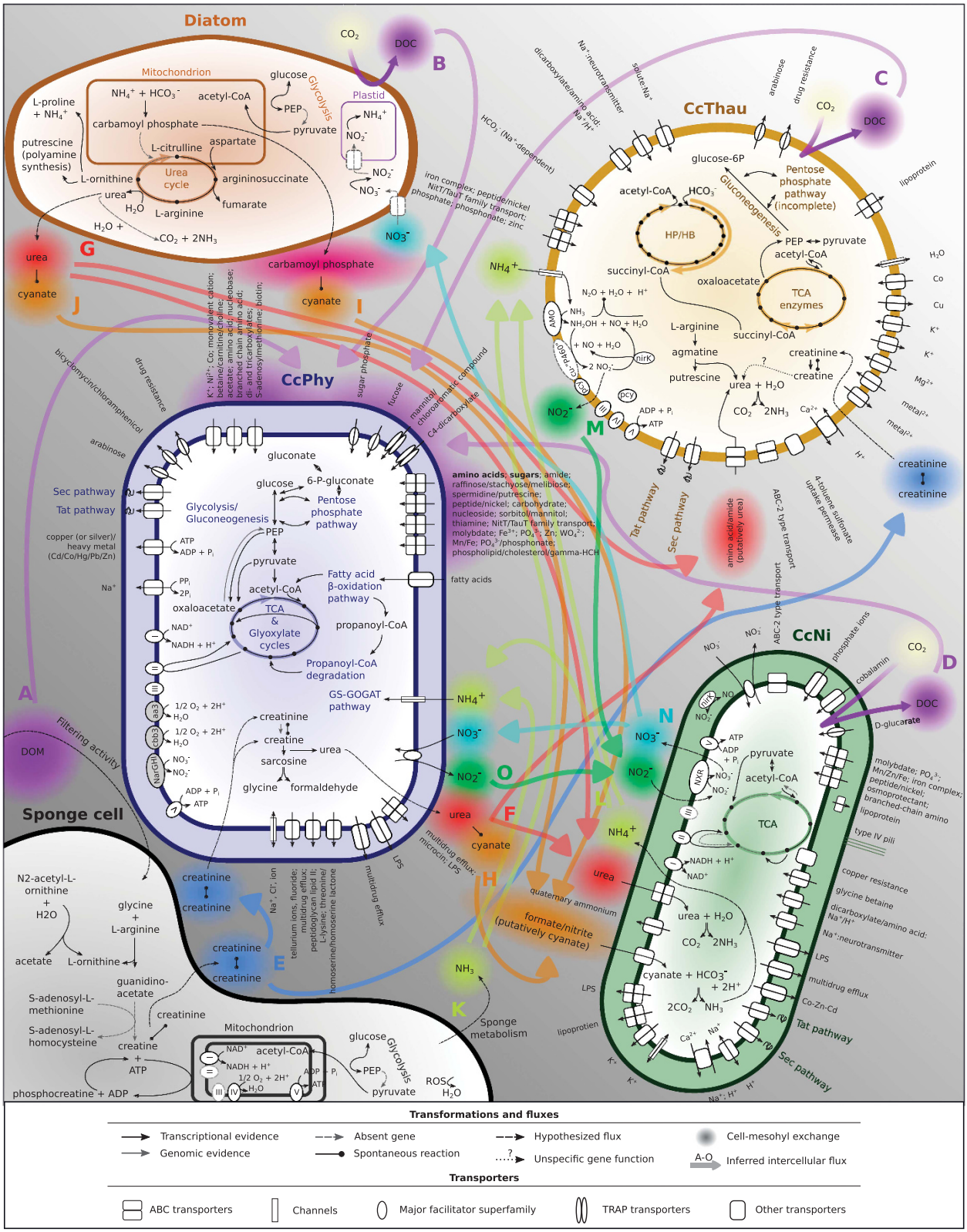

Figure 1 Predicted model of integrated metabolic processes within *Cymbastela concentrica*. Selected pathways and gene functions are shown. Transporters with at least partial genomic evidence and expression detected were included. Inferred nutrient fluxes (A–O) are discussed in the section 'Model of integrated metabolism of the microbial community members in *C. concentrica*'. Expressed genes are listed in Supplementary Tables S2.

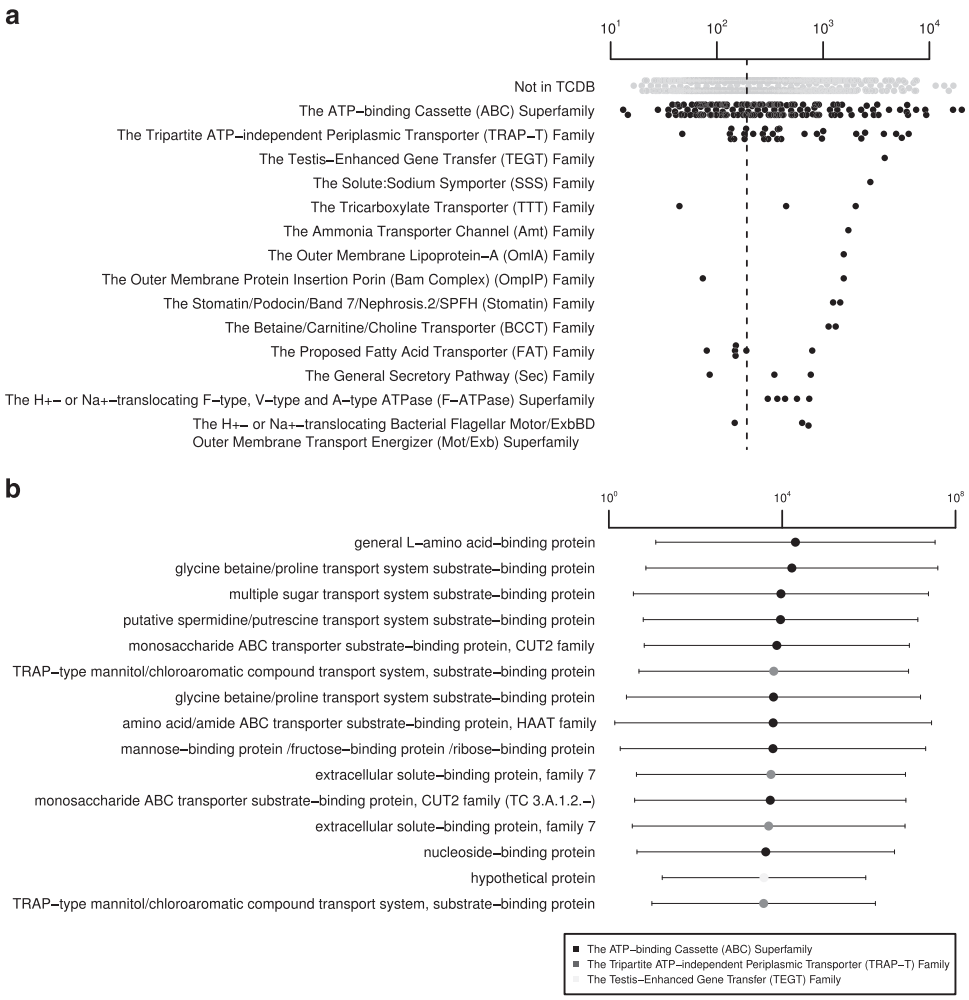

Figure 2 Most expressed CcPhy genes related to membrane transport. (**a**) CDS assigned to TCDB were grouped by families and super families. Groups were ordered according to maximum TPM_{av} values (*x* axis), and only the top 15 are shown. For reference, CDS not classified by TCDB are shown (not in TCDB). The median of all expressed genes is represented by the dashed line. (**b**) Most expressed transport-related genes. Gray scale refer to gene family or superfamily. Genes are ordered according to TPM_{av} values (*x* axis). Whiskers represent s.d. of biological replicates ($n = 3$).

levels for the aerobic, microaerobic and anaerobic respiratory pathways (Supplementary Figure S8). It is unlikely that any given individual cell within a population performs all three modes of respiration at the same time and therefore our observation indicates that subpopulations within the sponge tissue experience distinct oxygen environments.

Nitrite-dependent chemolithoautotrophy and use of organic nitrogen compounds by CcNi

Nitrospira are known to obtain energy by oxidizing nitrite to nitrate using the key enzyme nitrite oxidoreductase (NXR) (Spieck and Bock, 2005). The NXR of *Nitrospira* was proposed to be a membrane-bound periplasmic complex composed of at least two subunits, the subunits alpha (nxrA) and beta (nxrB) (Spieck *et al.*, 1998; Lucker *et al.*, 2010). Two adjacent genes encoding for nxrA (gene locus Ga0068443_101117) and nxrB (Ga0068443_101118) were found in CcNi (see Supplementary Information for phylogenetic analysis) representing the fourth and second most abundant transcripts in CcNi transcriptome (TPM_{av} 17 252 ± 9822 and TPM_{av} 26 308 ± 13 520, respectively; Figure 3). Electron transport and ATPase encoding genes were also expressed (Supplementary Table S2), supporting a nitrite-dependent chemolithotrophic electron flow (Lucker *et al.*, 2010). Expressed genes related to other nitrogen transformations were also found and are discussed in Supplementary Information. Taken together, these results indicate an active chemolithotrophic conversion of nitrite to nitrate by the CcNi population (Figure 1).

Few *Nitrospira* species can decompose urea using the resulting ammonia for nitrification and biomass production, where urea would be imported from the extracellular milieu by the urea ABC transporter and hydrolyzed by urease (Koch *et al.*, 2015; van Kessel *et al.*, 2015). CcNi possess an putative operon with genes related to the transport and decomposition of urea, including those encoding for subunits of

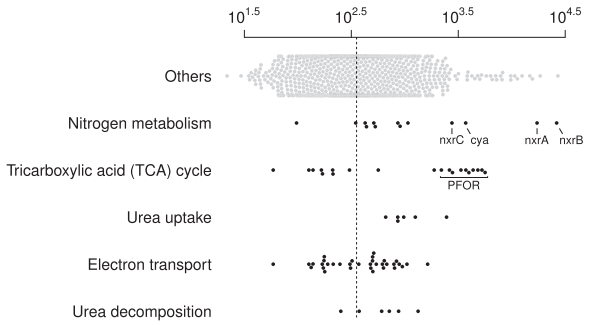

Figure 3 Expression of selected functional genes of CcNi. TPM_{av} values are shown for genes of selected functions. 'Others' stands for genes not grouped in the specific functions shown. The median of all expressed genes is represented by the dashed line. Highlighted genes encode for the nitrite oxidoreductase alpha (nxrA), beta (nxrB), putative C (nxrC) subunits (Supplementary Information), cyanate lyase (cya) and pyruvate ferredoxin oxidoreductase (PFOR).

urease, urea ABC transporter, as well as auxiliary proteins (Ga0068443_100614-16, Ga0068443_100619-27) (Supplementary Figure S9). Some of these genes were highly expressed, such as gene for the urtA urea transport system substrate-binding protein (TPM_{av} 2458 ± 357), the urease subunit alpha (TPM_{av} 1332 ± 420) and the urtD and urtE urea transport system ATP-binding proteins (TPM_{av} 978–1255; Figure 3). We did not find genomic evidence for the internal production of urea by CcNi, such as genes encoding for agmatinase or arginase. Because nitrite-oxidizing bacteria encode urea-producing enzymes (Palatinszky *et al*., 2015), the possibility of *Nitrospira*-like genes encoding for agmatinase or arginase to be expressed in *C. concentrica* was investigated. Transcripts encoding for sequences similar to agmatinase or arginase were found in the metatranscriptome of *C. concentrica* (Díez-Vives *et al*., 2016), but none of them were related to *Nitrospira* (Supplementary Information; Supplementary Table S4). This result further supports the absence of pathways for internal production of urea in CcNi.

The gene encoding for cyanate lyase (*cya*) was abundantly expressed in the transcriptome (TPM_{av} 3712 ± 1501) of CcNi (Figure 3). Cyanate lyase decomposes cyanate to CO_2 and ammonia in a reaction dependent of bicarbonate (Johnson and Anderson, 1987). Its activity was described in *N. moscoviensis* and its proposed biological roles include nitrogen assimilation, cyanate detoxification and energy acquisition (Anderson *et al*., 1990; Palatinszky *et al*., 2015). The *cya* gene was localized downstream from two genes encoding for proteins of the formate/nitrite transporter family (TPM_{av} 513–904) (Supplementary Figure S9). Members of the formate/nitrite transporter family (TC 2.A.44) have broad specificity for small monovalent anions (Lu *et al*., 2013). It is likely that CcNi putative formate/nitrite transporter is also permeable to cyanate, as similarly inferred for the ammonia-oxidizing archaea *Candidatus* Nitrososphaera gargensis due to the proximity of genes for transporter and enzymatic degradation (Spang *et al*., 2012).

Nitrospira species are proposed to fix carbon via the reductive TCA (rTCA) cycle (Starkenburg *et al*., 2006; Lucker *et al*., 2010, 2013; Koch *et al*., 2015). The rTCA cycle shares most of its enzymes with the oxidative TCA (oTCA) cycle, with the exception of three key enzymes, which are characteristic of the reductive cycle: ATP citrate lyase, 2-oxoglutarate: ferredoxin oxidoreductase (also named as α-ketogluterate synthase), and fumarate reductase (Berg, 2011). Alternatively, ATP-dependent cleavage of citrate can be carried by citryl-CoA synthetase and citryl-CoA lyase enzymes (Aoshima *et al*., 2004a, b). CcNi encoded enzymes that are shared between the two forms of TCA cycles. In addition, CcNi encoded a pyruvate ferredoxin oxidoreductase, which can act as pyruvate synthase (EC 1.2.7.1), carboxylating acetyl-CoA to pyruvate (Evans *et al*., 1966; Furdui and Ragsdale, 2000) (Figure 3). However, the characteristic rTCA key enzymes were not annotated in the genome (Figure 1). The annotation of genes encoding for A, B and C subunits of succinate dehydrogenase (complex II) or fumarate reductase (Ga0068443_100221-23) could indicate fumarate reductase activity and be considered an evidence for the rTCA cycle. These two enzymes are structurally similar and carry opposite reactions, that is, succinate oxidation and fumarate reduction (Hagerhall, 1997). Succinate dehydrogenase/fumarate reductase subunit genes are localized immediately adjacent to citrate synthase gene (Ga0068443_100220) in the CcNi genome. Although the mapping of metatranscriptomic reads to CDS does not allow us to verify whether they are co-expressed as an operon, their adjacent localization and similar expression levels (TPM_{av} 58–169) are suggestive of the participation of succinate dehydrogenase/fumarate reductase in the oTCA cycle as succinate dehydrogenase and not fumarate reductase. In the absence of evidence of other carbon fixation pathways (Supplementary Information), we hypothesize that CcNi fix carbon via rTCA cycle as conducted by other *Nitrospira* members, despite the lack of the key genes of this pathway in the genome bin.

Ammonia-dependent chemolithoautotrophy and use of organic nitrogen compounds by CcThau

Cultured members of the *Thaumarchaeota* are able to aerobically oxidase ammonia to nitrite (Stieglmeier *et al*., 2014a). Genes related to energy acquisition through ammonia oxidation were among the most abundantly transcribed in CcThau (TPM_{av} 3566–31 115, Figures 1 and 4). Ammonia oxidation is carried by ammonia monooxygenase, which in bacteria is composed of three subunits encoded by *amoA*, *amoB* and *amoC* genes (Arp *et al*., 2007). Additionally, a gene named '*amoX*' was proposed to be associated with the archaeal ammonia monooxygenase, due to

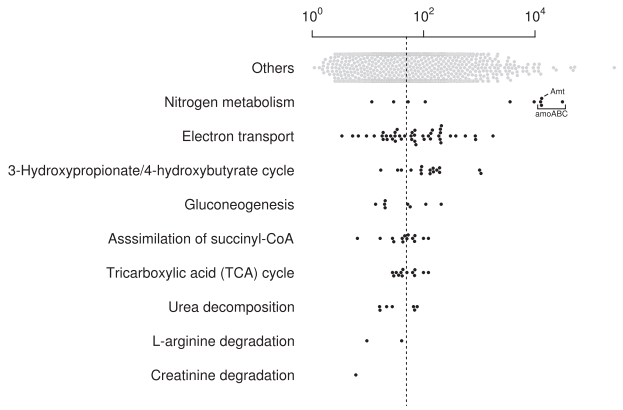

Figure 4 Expression of selected functional genes of CcThau. TPM_{av} values are shown for genes of selected functions. 'Others' stands for genes not grouped in the specific functions shown. The median of all expressed genes is represented by the dashed line. Highlighted genes encode for the ammonia monooxygenase subunits alpha (amoA), beta (amoB) and C (amoC) subunits as well as ammonium transporter (Amt).

the conserved co-localization with the subunit genes across ammonia-oxidizing archaea (Bartossek *et al.*, 2012). Single copies of genes putatively related to archaeal ammonia monooxygenase were present in pairs, amoA–amoX (Ga0078905_11462, Ga0078905_11463) and amoB–amoC (Ga0078905_103916-17), in the edge of two contigs, possibly forming a single gene array (*amoAXCB*) as observed in the genomes of *Nitrosoarchaeum limnia* SFB1 and *Nitrosopumilus maritimus* SCM1 (Walker *et al.*, 2010; Blainey *et al.*, 2011; Bartossek *et al.*, 2012). The gene encoding for an ammonium transporter (Ga0078905_100724, TPM_{av} 13 184 ± 1736) was estimated to be expressed at an approximate ratio of 1:1 to *amoA*. In addition, several genes putatively involved in ammonia-dependent chemolithotrophy in *Thaumarchaeota* were expressed at different levels by CcThau (Kozlowski *et al.*, 2016), including genes encoding for nitrite reductase (NO-forming) (TPM_{av} 107–9653), plastocyanins (TPM_{av} 37–1761), copper-binding proteins of the plastocyanin/azurin family (TPM_{av} 19–200), ubiquinol–cytochrome *c* reductase cytochrome *b* subunit (TPM_{av} 304 ± 26), multicopper oxidase (TPM_{av} 18 ± 4) and ATPase subunits (TPM_{av} 26–847). These findings are consistent with the observation of a large transcriptional effort invested in genes related to ammonia-dependent chemolithotrophy by archaeal populations in marine sponges (Radax *et al.*, 2012; Moitinho-Silva *et al.*, 2014).

Genomic analysis of several Thaumarchaea species revealed the presence of genes related to transport, production and degradation of urea (Palatinszky *et al.*, 2015). Urea can be used by *Thaumarchaeota* members as source of ammonia, as shown by biochemical assays of cultivated species (Lehtovirta-Morley *et al.*, 2016), and as carbon source, as inferred from ^{14}C-labeled urea incorporation of prokaryotic communities of Artic waters (Alonso-Saez *et al.*, 2012). The genes encoding for urease subunits, as well as auxiliary proteins, were present in two separate contigs of CcThau but lowly expressed (TPM_{av} 16–77). No encoded urea transporter was found. A set of genes encoding for amino acid/amide ABC transporter of the hydrophobic amino-acid uptake transporter (HAAT) family (TCDB:3.A.1.4), which includes urea transporters (Hosie *et al.*, 2002), were found in the genome. Thus it is conceivable that the encoded products may participate in urea transport. Urea can also be internally produced from the degradation of the amino-acid L-arginine (Shaibe *et al.*, 1985), and the genes encoding for arginine decarboxylase and agmatinase were expressed at low levels (TPM_{av} 10–40).

The expression of a gene encoding for creatinine amidohydrolase, albeit at low levels (TPM_{av} 6 ± 7), further indicates that CcThau degrades creatinine. Creatinine amidohydrolase genes are also present in other members of the candidate order *Nitrosopumilales*, for example, *Nitrosopumilus maritimus* SCM1 (Nmar_0222) (Walker *et al.*, 2010). The gene encoding for a creatinase, which would carry the downstream hydrolysis of creatine to sarcosine and urea (Shimizu *et al.*, 1986), was however not found in the CcThau genome bin. The most similar sequence to characterized creatinases from bacteria species was a gene encoding for a Xaa-Pro aminopeptidase (Ga0078905_10021), which is structurally related to creatinase (Supplementary Information; Supplementary Table S5; Bazan *et al.*, 1994). This similarity, however, does not provide enough evidence that CcThau converts creatinine to creatine in order to produce urea and, consequently, ammonia. Therefore, it is unclear in which biochemical context creatinine degradation is carried out by CcThau.

An almost complete set of genes for the 3-hydroxypropionate/4-hydroxybutyrate (HP/HB) pathway was expressed (Figure 1; Supplementary Table S2). The HP/HB pathway is an autotrophic CO_2 fixation cycle recently discovered in archaea and present in all *Thaumarchaeota* species characterized so far (Berg *et al.*, 2007; Bayer *et al.*, 2016). CcThau uses the same set of enzymes as *N. maritimus*, including 3-hydroxypropionyl-CoA synthetase (ADP-forming) (TPM_{av} 173 ± 53) and 4-hydroxybutyryl-CoA synthetase (ADP-forming) (TPM_{av} 90 ± 31) (Konneke *et al.*, 2014). In one cycle of the HP/HB pathway, two bicarbonate molecules are converted to one acetyl-coA. It is possible that the CcThau HP/HB pathway mainly connects to the central carbon metabolism via succinyl-CoA, which is produced from the generated acetyl-CoA and another pair of bicarbonate molecules by an additional half turn of the cycle (Estelmann *et al.*, 2011). With the exception of the gene for fumarase, for which no orthologous was identified, CcThau showed the expression of the enzymatic repertoire capable to further transform succinyl-coA into precursor metabolites, such as oxaloacetate,

phosphoenolpyruvate (PEP), pyruvate and 2-oxoglutarate (TPM_{av} 6–122). This set includes enzymes that are components of the oxidative TCA cycle. In addition, genes encoding for enzymes of the rTCA cycle were also found expressed, such as citrate lyase subunit beta/citryl-CoA lyase and 2-oxoglutarate ferredoxin oxidoreductase (TPM_{av} 32–39). In *Thaumarchaeota*, oTCA cycle was assumed to be used for anaplerotic reactions and the capacity of *Thaumarchaeota* to fix carbon via rTCA cycle was not demonstrated (Spang *et al.*, 2012; Zhalnina *et al.*, 2014; Stieglmeier *et al.*, 2014a). Mixotrophic growth has been reported in the *Thaumarchaeota* phylum (for example, Qin *et al.*, 2014). For CcThau, the possible uptake of urea and amino acids by the amino acid/amide ABC transporter of the HAAT family and the degradation of creatinine by creatinine amidohydrolase were the only evidence to suggest the use of external organic carbon sources (Supplementary Information).

Metabolic features of diatoms and the sponge

From the 184 053 eukaryotic transcripts recovered from *C. concentrica* (Díez-Vives *et al.*, 2016), the number of transcripts assigned to diatoms (*Bacillariophyta*) was similar to the combined number of transcripts classified as *Porifera* or as metazoans with best BLAST hit against sequences from sponges (Figure 5a). Higher expression, estimated from the sum of TPM values, was found for the host compared with the diatom symbiont (Figure 5b). Most transcripts could not be functionally classified for both organisms. Environmental information processing, genetic information processing and metabolism were the pathways with highest overall sums of TPM (Figure 5c). The comprehensive description of the diatom and sponge transcriptomes is beyond the scope of this study and therefore we focused here on key metabolic pathways.

The diatom symbionts invested a large transcriptional effort in functions for energy harvesting via photosynthesis and consumption via glycolysis (Figure 6a; Supplementary Table S6). In addition, functions related to arginine and proline metabolism were found to be abundantly expressed by the diatoms, in particular prolyl 4-hydroxylase (TPM_{sum} 46, Supplementary Table S6), the enzyme that carries out posttranslational modifications of proline (Gorres and Raines, 2010). The expression of carbamoyl-phosphate synthase, argininosuccinate synthase, argininosuccinate lyase and arginase (TPM_{sum} 3–10) are indicative of an active urea cycle in the diatom symbionts. Additional support for this metabolic cycle is provided by the expression of ornithine cyclodeaminase (TPM_{sum} 4) and ornithine decarboxylase (TPM_{sum} 5), which produce proline and putrescine from ornithine, respectively. The urea cycle in diatoms is proposed to redistribute and turnover inorganic carbon and nitrogen coming from catabolism and/or photorespiration (Allen *et al.*, 2011). With respect to sources of nitrogen, the diatoms expressed functions related to nitrate assimilation (nitrate reductase (NADPH), ferredoxin-nitrite

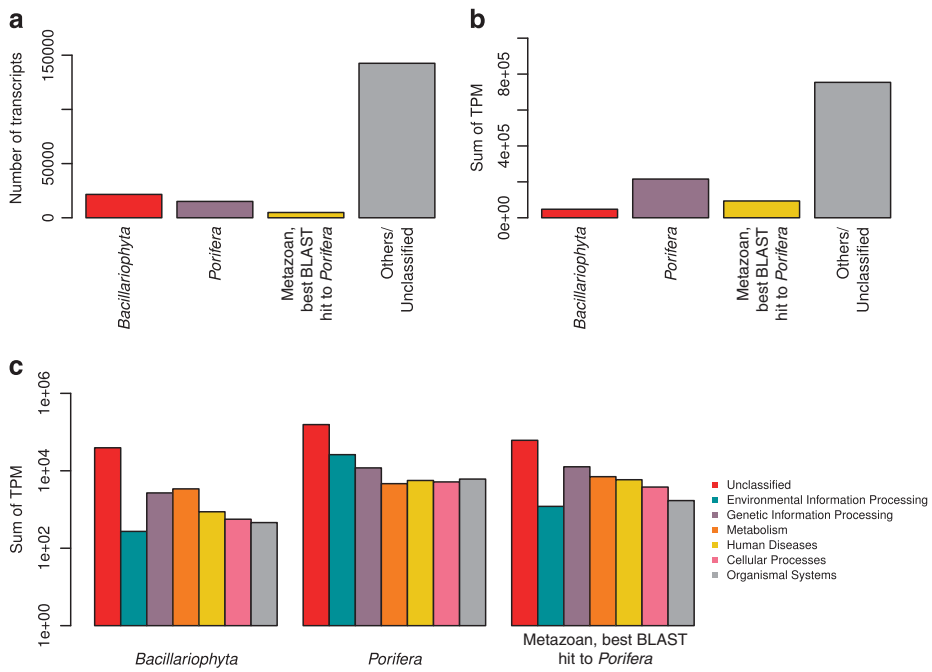

Figure 5 Expression of diatom and sponge transcripts in *Cymbastela concentrica*. (**a**) Transcripts taxonomically classified as diatoms (*Bacillariophyta*) or sponge (*Porifera* or Metazoan with best BLAST hit to sponge sequences) were sorted from other eukaryotic transcripts recovered from *C. concentrica*. (**b**) Overall expression of diatom and sponge is indicated by the sum of transcripts' TPM. (**c**) Deduced peptide sequences from transcripts' coding sequences were used for KEGG functional classification. Expression of KEGG functions was inferred from the sum of TPM values across coding sequences.

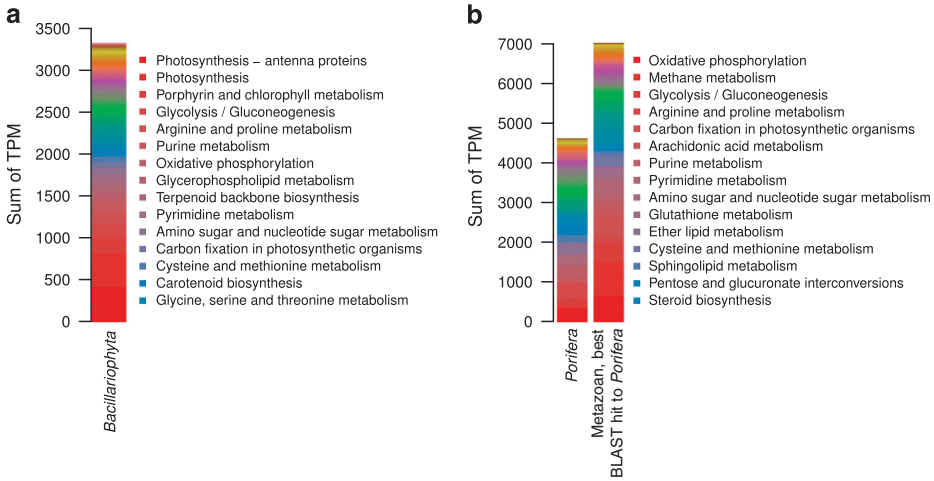

Figure 6 Expressed metabolic functions in diatoms and the sponge. Sums of TPM are shown for KEGG metabolic pathways found in (**a**) diatoms (*Bacillariophyta*) and (**b**) sponge (*Porifera* and Metazoan or Metazoan with best BLAST hit to sponge sequences). Legends list the top expressed pathways.

reductase, TPM_{sum} 2–5) and production of ammonia via nitrite generated from the oxygenation of alkyl nitronates (nitronate monooxygenase TPM_{sum} 1). The co-expression of these pathways at different intensities has also been recently observed in metatranscriptomes of *Skeletonema* spp. recovered from surface seawater (Alexander *et al.*, 2015) and indicates the simultaneous use of multiple sources of nitrogen by the diatom symbiont.

Sponge cells abundantly expressed functions of the oxidative phosphorylation (for example, cytochrome *c* oxidase subunit 6a, TPM_{sum} 418, Supplementary Table S7) and glycolysis (glyceraldehyde 3-phosphate dehydrogenase, TPM_{sum} 418) (Figure 6b). The expression of functions assigned to methane metabolism was largely due to antioxidant enzymes, catalase (TPM_{sum} 468) and peroxiredoxin 6, 1-Cys peroxiredoxin (TPM_{sum} 353), which may protect the sponge cells from reactive oxygen species (Tate *et al.*, 1995; Chen *et al.*, 2000). The most abundant functions related to arginine and proline metabolism were acetylornithine deacetylase (TPM_{sum} 237) and glycine amidinotransferase (TPM_{sum} 94). Both enzymes carry out reactions that produces L-ornithine, the former from N2-acetyl-L-ornithine and H_2O and the latter from L-arginine and glycine. The reaction of glycine amidinotransferase is the first of the two-step creatine biosynthesis (Wyss and Kaddurah-Daouk, 2000). Along with creatine, creatinine is expected to be found in sponge cells, as it is a product of spontaneous, non-enzymatic conversion of the former. In addition, the sponge expressed a creatine kinase function (TPM_{sum} 34), which reversibly converts creatine and ATP to phosphocreatine and ADP. This result is in support of previous detection of creatine kinase activity in the tissue of the sponge *Tethya aurantia* (Ellington, 2000; Sona *et al.*, 2004). In sponges, the creatine kinase/phosphocreatine system was proposed as an intracellular spatial buffer of energy, connecting the ATP produced in the mitochondria with distant cytosolic sites of ATP consumption (Sona *et al.*, 2004; Ellington and Suzuki, 2007).

Model of integrated metabolism of the microbial community members in C. concentrica

Based on the genomic and transcriptomic information of these three prokaryotic symbionts and the expression of eukaryotic transcripts assigned to diatoms and sponges, we developed a metabolic model for the sponge–microbe symbiosis in which nutrient fluxes between cells and the extracellular milieu, that is the sponge mesohyl, were inferred from our data set (see Figure 1).

As shown above, CcPhy is a heterotrophic bacterium with the capacity to uptake a range of organic and inorganic compounds. Such nutrients are likely found across the sponge tissue, which is consistent with a scattered distribution of CcPhy cells throughout the mesohyl (see Figure 7; Supplementary Figure S10). Considering the high relative abundance of *Phyllobacteriaceae* within the symbiont community (Fan *et al.*, 2012; Esteves *et al.*, 2016), CcPhy may thus be a major contributor to uptake and utilization of DOM by the microbiome. The DOM used by CcPhy may come from the sponge's filtering activity (Figure 1a; de Goeij *et al.*, 2008, 2013) or from diatoms (Figure 1b) that were found throughout the mesohyl (Figure 7), especially considering that axenic cultures of diatoms have been shown to release between 5% and 21% of their total fixed carbon as dissolved organic carbon (Wetz and Wheeler, 2007). In support of this, photosynthesis functions were abundantly expressed in the diatom transcriptome (Figure 6a). Another source of carbon for the members of the sponge–microbe symbiosis may be from the autotrophic metabolism of CcThau and CcNi (Figures 1c and d, see above).

Creatine and creatinine are products of the sponge metabolism, as indicated by the expression

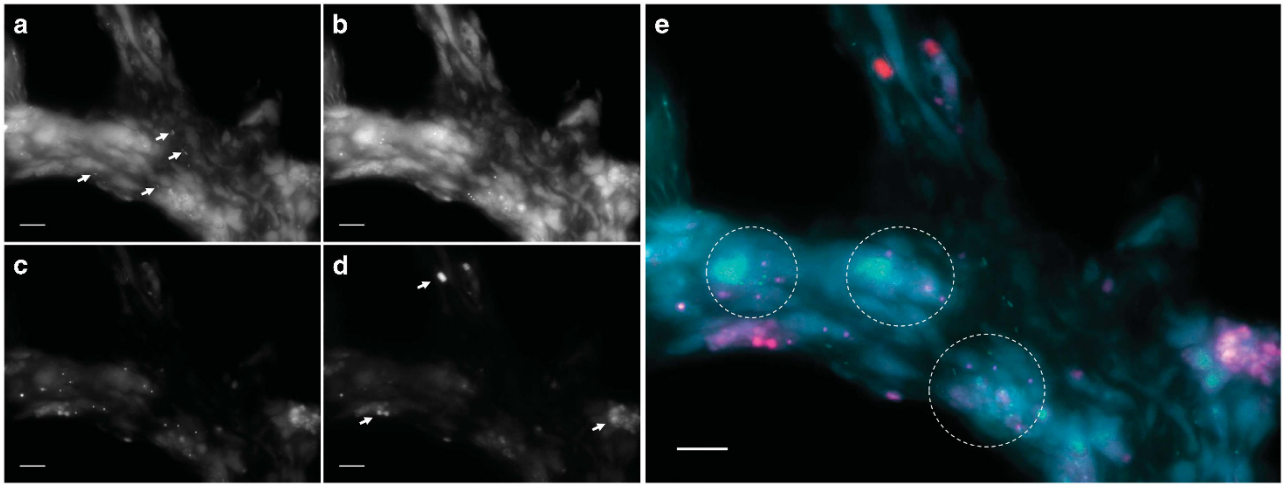

Figure 7 Visualization of microorganisms associated with *Cymbastela concentrica* by fluorescence *in situ* hybridization. (**a**) Rod-shaped cells (white arrows) were observed from hybridization with a Pacific Blue-labeled CcPhy-specific probe. Signals from (**b**) fluorescein-isothiocyanate-labeled CcNi-specific and (**c**) Cy3-labeled CcThau-specific probes are shown. (**d**) Red autofluorescence signals from diatoms were captured (arrows). (**e**) Clusters of CcNi-specific (green) and CcThau-specific (magenta) probes in the sponge mesohyl are highlighted in the merged color image by circles. CcPhy cells (cyan) did not specifically co-localize with CcNi or CcThau cells. Autofluorescence of the sponge tissue (light blue/cyan) served as a reference for the structure of the sponge mesohyl. Scale bars, 10 μm.

transcripts encoding for glycine amidinotransferase and creatine kinase. Although it is unknown whether sponge cells exchange creatine between different cells and tissues as described in higher animals (Wyss and Kaddurah-Daouk, 2000), it is conceivable that these compounds are accessible to the microbial community (Figure 1e). The possibility that creatine and creatinine are actively used by the microbiome is supported by the expression of genes able to degrade creatine to glycine by CcPhy and the encoded creatinine amidohydrolase in CcPhy and CcThau genomes. The degradation of these host metabolites by the symbionts is likely widespread, as inferred by the previous observation of related genes in the metagenome of six sponges, including *C. concentrica* (Fan *et al.*, 2012). Here we could assign this function to be actively used by specific members of the microbiome.

The metabolism of CcPhy, diatom, CcNi and CcThau are linked by the production and consumption of urea. CcPhy internally generates urea from creatine degradation, which can potentially accumulate and diffuse through the bacterial membrane (Figure 1f; Lodish *et al.*, 2000). This assumption is further supported by the fact that heterotrophic marine bacteria have been observed to be net producer of urea even in the presence of hydrolytic activity (Cho *et al.*, 1996; Berg and Jorgensen, 2006). The diatom symbiont is another potential source of urea as suggested by the expression of the urea cycle (Figure 1g). The *Nitrospira* population represented by CcNi may benefit directly from the urea in the extracellular milieu, as it abundantly expresses the genes related to the transport and degradation of urea. Despite the internal production of urea via L-arginine degradation, CcThau may also uptake urea via the amino acid/amide ABC transporter of the HAAT family. Additionally, urea can spontaneously dissociate to cyanate (Marier and Rose, 1964; Guilloton and Karst, 1985). Similarly, cyanate is formed from carbamoyl phosphate (Allen and Jones, 1964), which is an intermediate of the urea cycle in diatoms. Therefore, urea indirectly links CcPhy and the diatom symbiont to CcNi via cyanate (Figures 1h–j), which could be imported and decomposed to CO_2 and ammonia as indicated by the expression of cyanate lyase genes in CcNi.

Urease genes were also found in other sponge-associated microbial genomes and microbiomes (Hallam *et al.*, 2006; Siegl *et al.*, 2011; Bayer *et al.*, 2014; Liu *et al.*, 2016). Together with the phylogenetic diversity found for *ureC* genes and transcripts found in the sponge *Xestospongia testudinaria* (Su *et al.*, 2013), these data indicate that urea degradation is a common trait of sponge-associated microorganisms. Although urea can be found in benthic environments (Crandall and Teece, 2012), our data points to the possibility of urea being derived from host metabolites, that is, via bacterial metabolism of creatine and creatinine, and from intracellular metabolism of sponge symbionts, such as diatoms.

Pumping activity and host metabolism have been regarded as sources of ammonia in the sponge tissue (Ribes *et al.*, 2012; Figure 1k). Additionally, urea and cyanate are degraded by CcNi, which is likely a source of ammonia (Figure 1l; Koch *et al.*, 2015). Our analysis indicates that CcPhy takes up ammonium for nitrogen assimilation, while CcThau oxidizes ammonia to generate energy, releasing nitrite (Figure 1m). Nitrite in turn serves as the energy source for CcNi, which expressed the genes necessary for nitrite oxidation. Fluorescence *in situ* hybridization analysis showed that CcThau and CcNi are often localized in close proximity (Figure 7), supporting such a metabolic interaction. Nitrification, a process in which the oxidation of ammonia is coupled with the oxidation of nitrite, is a common

theme in sponge microbiology, being the subject of many studies (Taylor *et al.*, 2007). Based on the use of urea and cyanate as indirect sources of ammonia in nitrification carried out by co-cultures of *Nitrospira* and ammonia-oxidizing bacteria (Koch *et al.*, 2015; Palatinszky *et al.*, 2015) and the expression profile of CcNi and CcThau, we propose that these compounds should be considered when modeling nitrification in marine sponges.

The end product of the combined aerobic nitrification by CcThau and CcNi is nitrate, which would support anaerobic nitrate respiration by CcPhy (Figure 1n, see above). Such a coupling is possible if the two processes and their associated population are temporally and/or spatially separated by variations in oxygen concentration or redox potential, which have been described to occur in sponges (Schläppy *et al.*, 2010; Lavy *et al.*, 2016). The facultative nature of the CcPhy metabolism supports its temporal separation from the aerobic metabolisms CcThau and CcNi, while the observation that CcPhy rarely co-occured with the CcThau and CcNi cells would indicate also a spatial separation of their metabolisms (see Figure 7). The incomplete denitrification pathway of CcPhy would also yield nitrite (Figure 1o), which again could serve as an energy source for CcNi, thus creating a 'mini' N cycle at the interface of aerobic and anaerobic micro-habitats. An alternative path for the N cycle within *C. concentrica* is the nitrate assimilation by diatoms (Figure 1n).

Conclusion

We described the lifestyle of prominent members of *C. concentrica* sponge–microbe symbiosis, that is, associated prokaryotes, diatoms and the host, by analyzing their transcriptional activities. Although connected metabolic pathways are expected to occur based on the complexity of nutrient cycles within sponges (Hoffmann *et al.*, 2009), our study is unprecedented in modeling how the physiology of microbiome members are integrated. We thus predicted how and which members can generate, retain, recycle and compete for biochemical resources. In addition, we considered the gene expression of the sponge and diatoms, unveiling the nutritional basis for biological interactions within the sponge–microbe symbiosis. Finally, we demonstrated the power of a holistic approach to further our understanding of the complexity of animal–microbe symbioses.

Conflict of Interest

The authors declare no conflict of interest.

Acknowledgements

We acknowledge the financial support of the Betty and Gordon Moore Foundation and the Australian Research Council. We thank Dr Tamsin Peters and Jadranka Nappi for sample collection. We also thank Dr Ute Hentschel for hosting GB at the GEOMAR Helmholtz Centre for Ocean Research. MTJ was supported by grants of the German Excellence Initiative to the Graduate School of Life Sciences, University of Wuerzburg.

References

Alexander H, Jenkins BD, Rynearson TA, Dyhrman ST. (2015). Metatranscriptome analyses indicate resource partitioning between diatoms in the field. *Proc Natl Acad Sci USA* **112**: E2182–E2190.

Allen AE, Dupont CL, Obornik M, Horak A, Nunes-Nesi A, McCrow JP *et al.* (2011). Evolution and metabolic significance of the urea cycle in photosynthetic diatoms. *Nature* **473**: 203–207.

Allen CM, Jones ME. (1964). Decomposition of carbamylphosphate in aqueous solutions. *Biochemistry* **3**: 1238–1247.

Alonso-Saez L, Waller AS, Mende DR, Bakker K, Farnelid H, Yager PL *et al.* (2012). Role for urea in nitrification by polar marine Archaea. *Proc Natl Acad Sci USA* **109**: 17989–17994.

Anderson PM, Sung YC, Fuchs JA. (1990). The cyanase operon and cyanate metabolism. *FEMS Microbiol Rev* **7**: 247–252.

Aoshima M, Ishii M, Igarashi Y. (2004a). A novel enzyme, citryl-CoA synthetase, catalysing the first step of the citrate cleavage reaction in *Hydrogenobacter thermophilus* TK-6. *Mol Microbiol* **52**: 751–761.

Aoshima M, Ishii M, Igarashi Y. (2004b). A novel enzyme, citryl-CoA lyase, catalysing the second step of the citrate cleavage reaction in *Hydrogenobacter thermophilus* TK-6. *Mol Microbiol* **52**: 763–770.

Arp DJ, Chain PS, Klotz MG. (2007). The impact of genome analyses on our understanding of ammonia-oxidizing bacteria. *Annu Rev Microbiol* **61**: 503–528.

Bartossek R, Spang A, Weidler G, Lanzen A, Schleper C. (2012). Metagenomic analysis of ammonia-oxidizing archaea affiliated with the soil group. *Front Microbiol* **3**: 208.

Bayer B, Vojvoda J, Offre P, Alves RJ, Elisabeth NH, Garcia JA *et al.* (2016). Physiological and genomic characterization of two novel marine thaumarchaeal strains indicates niche differentiation. *ISME J* **10**: 1051–1063.

Bayer K, Moitinho-Silva L, Brummer F, Cannistraci CV, Ravasi T, Hentschel U. (2014). GeoChip-based insights into the microbial functional gene repertoire of marine sponges (high microbial abundance, low microbial abundance) and seawater. *FEMS Microbiol Ecol* **90**: 832–843.

Bazan JF, Weaver LH, Roderick SL, Huber R, Matthews BW. (1994). Sequence and structure comparison suggest that methionine aminopeptidase, prolidase, aminopeptidase P, and creatinase share a common fold. *Proc Natl Acad Sci USA* **91**: 2473–2477.

Bell JJ. (2008). The functional roles of marine sponges. *Estuar Coastal Shelf Sci* **79**: 341–353.

Berg GM, Jorgensen NOG. (2006). Purine and pyrimidine metabolism by estuarine bacteria. *Aquat Microb Ecol* **42**: 215–226.

Berg IA, Kockelkorn D, Buckel W, Fuchs G. (2007). A 3-hydroxypropionate/4-hydroxybutyrate autotrophic

carbon dioxide assimilation pathway in Archaea. *Science* **318**: 1782–1786.
Berg IA. (2011). Ecological aspects of the distribution of different autotrophic CO2 fixation pathways. *Appl Environ Microbiol* **77**: 1925–1936.
Bertero MG, Rothery RA, Palak M, Hou C, Lim D, Blasco F *et al.* (2003). Insights into the respiratory electron transfer pathway from the structure of nitrate reductase A. *Nat Struct Biol* **10**: 681–687.
Blainey PC, Mosier AC, Potanina A, Francis CA, Quake SR. (2011). Genome of a low-salinity ammonia-oxidizing archaeon determined by single-cell and metagenomic analysis. *PLoS ONE* **6**: e16626.
Cary SC, Giovannoni SJ. (1993). Transovarial inheritance of endosymbiotic bacteria in clams inhabiting deep-sea hydrothermal vents and cold seeps. *Proc Natl Acad Sci USA* **90**: 5695–5699.
Chen J-W, Dodia C, Feinstein SI, Jain MK, Fisher AB. (2000). 1-Cys peroxiredoxin, a bifunctional enzyme with glutathione peroxidase and phospholipase A2 activities. *J Biol Chem* **275**: 28421–28427.
Cho B, Park M, Shim J, Azam F. (1996). Significance of bacteria in urea dynamics in coastal surface waters. *Mar Ecol Prog Ser* **142**: 19–26.
Cho I, Blaser MJ. (2012). The human microbiome: at the interface of health and disease. *Nat Rev Genet* **13**: 260–270.
Coyte KZ, Schluter J, Foster KR. (2015). The ecology of the microbiome: networks, competition, and stability. *Science* **350**: 663–666.
Crandall JB, Teece MA. (2012). Urea is a dynamic pool of bioavailable nitrogen in coral reefs. *Coral Reefs* **31**: 207–214.
de Goeij JM, van den Berg H, van Oostveen MM, Epping EHG, van Duyl FC. (2008). Major bulk dissolved organic carbon (DOC) removal by encrusting coral reef cavity sponges. *Mar Ecol Prog Ser* **357**: 139–151.
de Goeij JM, van Oevelen D, Vermeij MJ, Osinga R, Middelburg JJ, de Goeij AF *et al.* (2013). Surviving in a marine desert: the sponge loop retains resources within coral reefs. *Science* **342**: 108–110.
Dethlefsen L, McFall-Ngai M, Relman DA. (2007). An ecological and evolutionary perspective on human-microbe mutualism and disease. *Nature* **449**: 811–818.
Díez-Vives C, Moitinho-Silva L, Nielsen S, Reynolds D, Thomas T. (2016). Expression of eukaryotic-like protein in the microbiome of sponges. *Mol Ecol*; e-pub ahead of print 30 December 2016; doi:10.1111/mec.14003.
Douglas AE, Werren JH. (2016). Holes in the hologenome: why host-microbe symbioses are not holobionts. *MBio* **7**: e02099.
Ellington WR. (2000). A dimeric creatine kinase from a sponge: implications in terms of phosphagen kinase evolution. *Comp Biochem Physiol B Biochem Mol Biol* **126**: 1–7.
Ellington WR, Suzuki T. (2007). Early evolution of the creatine kinase gene family and the capacity for creatine biosynthesis and membrane transport. *Subcell Biochem* **46**: 17–26.
Estelmann S, Hugler M, Eisenreich W, Werner K, Berg IA, Ramos-Vera WH *et al.* (2011). Labeling and enzyme studies of the central carbon metabolism in *Metallosphaera sedula*. *J Bacteriol* **193**: 1191–1200.
Esteves AI, Amer N, Nguyen M, Thomas T. (2016). Sample processing impacts the viability and cultivability of the sponge microbiome. *Front Microbiol* **7**: 499.
Evans MC, Buchanan BB, Arnon DI. (1966). A new ferredoxin-dependent carbon reduction cycle in a photosynthetic bacterium. *Proc Natl Acad Sci USA* **55**: 928–934.
Fan L, Reynolds D, Liu M, Stark M, Kjelleberg S, Webster NS *et al.* (2012). Functional equivalence and evolutionary convergence in complex communities of microbial sponge symbionts. *Proc Natl Acad Sci USA* **109**: E1878–E1887.
Freeman CJ, Thacker RW, Baker DM, Fogel ML. (2013). Quality or quantity: is nutrient transfer driven more by symbiont identity and productivity than by symbiont abundance? *ISME J* **7**: 1116–1125.
Furdui C, Ragsdale SW. (2000). The role of pyruvate ferredoxin oxidoreductase in pyruvate synthesis during autotrophic growth by the Wood-Ljungdahl pathway. *J Biol Chem* **275**: 28494–28499.
Gabel C, Maier RJ. (1993). Oxygen-dependent transcriptional regulation of cytochrome aa3 in *Bradyrhizobium japonicum*. *J Bacteriol* **175**: 128–132.
Garcia-Horsman JA, Barquera B, Rumbley J, Ma J, Gennis RB. (1994). The superfamily of heme-copper respiratory oxidases. *J Bacteriol* **176**: 5587–5600.
Gillan FT, Stoilov IL, Thompson JE, Hogg RW, Wilkinson CR, Djerassi C. (1988). Fatty acids as biological markers for bacterial symbionts in sponges. *Lipids* **23**: 1139–1145.
Gorres KL, Raines RT. (2010). Prolyl 4-hydroxylase. *Crit Rev Biochem Mol Biol* **45**: 106–124.
Guilloton M, Karst F. (1985). A spectrophotometric determination of cyanate using reaction with 2-aminobenzoic acid. *Anal Biochem* **149**: 291–295.
Hadas E, Shpigel M, Ilan M. (2009). Particulate organic matter as a food source for a coral reef sponge. *J Exp Biol* **212**: 3643–3650.
Hagerhall C. (1997). Succinate: quinone oxidoreductases. Variations on a conserved theme. *Biochim Biophys Acta* **1320**: 107–141.
Hallam SJ, Mincer TJ, Schleper C, Preston CM, Roberts K, Richardson PM *et al.* (2006). Pathways of carbon assimilation and ammonia oxidation suggested by environmental genomic analyses of marine Crenarchaeota. *PLoS Biol* **4**: e95.
Hoffmann F, Radax R, Woebken D, Holtappels M, Lavik G, Rapp HT *et al.* (2009). Complex nitrogen cycling in the sponge Geodia barretti. *Environ Microbiol* **11**: 2228–2243.
Hosie AH, Allaway D, Galloway CS, Dunsby HA, Poole PS. (2002). Rhizobium leguminosarum has a second general amino acid permease with unusually broad substrate specificity and high similarity to branched-chain amino acid transporters (Bra/LIV) of the ABC family. *J Bacteriol* **184**: 4071–4080.
Huson DH, Mitra S, Ruscheweyh HJ, Weber N, Schuster SC. (2011). Integrative analysis of environmental sequences using MEGAN4. *Genome Res* **21**: 1552–1560.
Imelfort M, Parks D, Woodcroft BJ, Dennis P, Hugenholtz P, Tyson GW. (2014). GroopM: an automated tool for the recovery of population genomes from related metagenomes. *PeerJ* **2**: e603.
Javelle A, Thomas G, Marini AM, Kramer R, Merrick M. (2005). *In vivo* functional characterization of the *Escherichia coli* ammonium channel AmtB: evidence for metabolic coupling of AmtB to glutamine synthetase. *Biochem J* **390**: 215–222.
Johnson WV, Anderson PM. (1987). Bicarbonate is a recycling substrate for cyanase. *J Biol Chem* **262**: 9021–9025.

Kamke J, Sczyrba A, Ivanova N, Schwientek P, Rinke C, Mavromatis K *et al.* (2013). Single-cell genomics reveals complex carbohydrate degradation patterns in poribacterial symbionts of marine sponges. *ISME J* **7**: 2287–2300.

Kikuchi Y, Hosokawa T, Fukatsu T. (2007). Insect-microbe mutualism without vertical transmission: a stinkbug acquires a beneficial gut symbiont from the environment every generation. *Appl Environ Microbiol* **73**: 4308–4316.

Kim JM, Shimizu S, Yamada H. (1986). Sarcosine oxidase involved in creatinine degradation in *Alcaligenes denitrificans* subsp *dentrificans* J9 and *Arthrobacter* spp J5 and J11. *Agric Biol Chem* **50**: 2811–2816.

Koch H, Lucker S, Albertsen M, Kitzinger K, Herbold C, Spieck E *et al.* (2015). Expanded metabolic versatility of ubiquitous nitrite-oxidizing bacteria from the genus *Nitrospira*. *Proc Natl Acad Sci USA* **112**: 11371–11376.

Konneke M, Bernhard AE, de la Torre JR, Walker CB, Waterbury JB, Stahl DA. (2005). Isolation of an autotrophic ammonia-oxidizing marine archaeon. *Nature* **437**: 543–546.

Konneke M, Schubert DM, Brown PC, Hugler M, Standfest S, Schwander T *et al.* (2014). Ammonia-oxidizing archaea use the most energy-efficient aerobic pathway for CO_2 fixation. *Proc Natl Acad Sci USA* **111**: 8239–8244.

Koopmans M, van Rijswijk P, Boschker HT, Marco H, Martens D, Wijffels RH. (2015). Seasonal variation of Fatty acids and stable carbon isotopes in sponges as indicators for nutrition: biomarkers in sponges identified. *Mar Biotechnol (NY)* **17**: 43–54.

Kozlowski JA, Stieglmeier M, Schleper C, Klotz MG, Stein LY. (2016). Pathways and key intermediates required for obligate aerobic ammonia-dependent chemolithotrophy in bacteria and Thaumarchaeota. *ISME J* **10**: 1836–1845.

Kraft B, Strous M, Tegetmeyer HE. (2011). Microbial nitrate respiration–genes, enzymes and environmental distribution. *J Biotechnol* **155**: 104–117.

Langmead B, Trapnell C, Pop M, Salzberg SL. (2009). Ultrafast and memory-efficient alignment of short DNA sequences to the human genome. *Genome Biol* **10**: R25.

Lavy A, Keren R, Yahel G, Ilan M. (2016). Intermittent hypoxia and prolonged suboxia measured in situ in a marine sponge. *Front Mar Sci* **3**: 263.

Lehtovirta-Morley LE, Ross J, Hink L, Weber EB, Gubry-Rangin C, Thion C *et al.* (2016). Isolation of '*Candidatus* Nitrosocosmicus franklandus', a novel ureolytic soil archaeal ammonia oxidiser with tolerance to high ammonia concentration. *FEMS Microbiol Ecol* **92**.

Li B, Ruotti V, Stewart RM, Thomson JA, Dewey CN. (2010). RNA-Seq gene expression estimation with read mapping uncertainty. *Bioinformatics* **26**: 493–500.

Li B, Dewey CN. (2011). RSEM: accurate transcript quantification from RNA-Seq data with or without a reference genome. *BMC Bioinformatics* **12**: 1–16.

Liu F, Li J, Feng G, Li Z. (2016). New genomic insights into 'Entotheonella' symbionts in *Theonella swinhoei*: mixotrophy, anaerobic adaptation, resilience, and interaction. *Front Microbiol* **7**: 1333.

Liu M, Fan L, Zhong L, Kjelleberg S, Thomas T. (2012). Metaproteogenomic analysis of a community of sponge symbionts. *ISME J* **6**: 1515–1525.

Liu MY, Kjelleberg S, Thomas T. (2011). Functional genomic analysis of an uncultured delta-proteobacterium in the sponge *Cymbastela concentrica*. *ISME J* **5**: 427–435.

Lodish H, Berk A, Zipursky SL, Matsudaira P, Baltimore D, Darnell J. (2000). *Section 15.1. Diffusion of Small Molecules Across Phospholipid Bilayers. Molecular Cell Biology*4th ednFreeman & Co.: New York, NY, USA, p1084.

Lu W, Du J, Schwarzer NJ, Wacker T, Andrade SL, Einsle O. (2013). The formate/nitrite transporter family of anion channels. *Biol Chem* **394**: 715–727.

Lucker S, Wagner M, Maixner F, Pelletier E, Koch H, Vacherie B *et al.* (2010). A Nitrospira metagenome illuminates the physiology and evolution of globally important nitrite-oxidizing bacteria. *Proc Natl Acad Sci USA* **107**: 13479–13484.

Lucker S, Nowka B, Rattei T, Spieck E, Daims H. (2013). The genome of nitrospina gracilis illuminates the metabolism and evolution of the major marine nitrite oxidizer. *Front Microbiol* **4**: 27.

Marier JR, Rose D. (1964). Determination of cyanate, and a study of its accumulation in aqueous solutions of urea. *Anal Biochem* **7**: 304–314.

Markowitz VM, Chen IM, Palaniappan K, Chu K, Szeto E, Pillay M *et al.* (2014). IMG 4 version of the integrated microbial genomes comparative analysis system. *Nucleic Acids Res* **42**: D560–D567.

Marta R, Rafel C, Josep-Maria G. (1999). Natural diet and grazing rate of the temperate sponge *Dysidea avara* (Demospongiae, Dendroceratida) throughout an annual cycle. *Mar Ecol Prog Ser* **176**: 179–190.

Martens EC, Heungens K, Goodrich-Blair H. (2003). Early colonization events in the mutualistic association between *Steinernema carpocapsae* nematodes and *Xenorhabdus nematophila* bacteria. *J Bacteriol* **185**: 3147–3154.

Moitinho-Silva L, Seridi L, Ryu T, Voolstra CR, Ravasi T, Hentschel U. (2014). Revealing microbial functional activities in the Red Sea sponge *Stylissa carteri* by metatranscriptomics. *Environ Microbiol* **16**: 3683–3698.

Morris RL, Schmidt TM. (2013). Shallow breathing: bacterial life at low O(2). *Nat Rev Microbiol* **11**: 205–212.

Palatinszky M, Herbold C, Jehmlich N, Pogoda M, Han P, von Bergen M *et al.* (2015). Cyanate as an energy source for nitrifiers. *Nature* **524**: 105–108.

Parks DH, Imelfort M, Skennerton CT, Hugenholtz P, Tyson GW. (2015). CheckM: assessing the quality of microbial genomes recovered from isolates, single cells, and metagenomes. *Genome Res* **25**: 1043–1055.

Peix A, Rivas R, Trujillo ME, Vancanneyt M, Velazquez E, Willems A. (2005). Reclassification of *Agrobacterium ferrugineum* LMG 128 as *Hoeflea marina* gen. nov., sp. nov. *Int J Syst Evol Microbiol* **55**: 1163–1166.

Preisig O, Zufferey R, Thony-Meyer L, Appleby CA, Hennecke H. (1996). A high-affinity cbb3-type cytochrome oxidase terminates the symbiosis-specific respiratory chain of *Bradyrhizobium japonicum*. *J Bacteriol* **178**: 1532–1538.

Qin W, Amin SA, Martens-Habbena W, Walker CB, Urakawa H, Devol AH *et al.* (2014). Marine ammonia-oxidizing archaeal isolates display obligate mixotrophy and wide ecotypic variation. *Proc Natl Acad Sci USA* **111**: 12504–12509.

Radax R, Rattei T, Lanzen A, Bayer C, Rapp HT, Urich T *et al.* (2012). Metatranscriptomics of the marine sponge Geodia barretti: tackling phylogeny and function of its microbial community. *Environ Microbiol* **14**: 1308–1324.

Ribes M, Jimenez E, Yahel G, Lopez-Sendino P, Diez B, Massana R *et al.* (2012). Functional convergence of microbes associated with temperate marine sponges. *Environ Microbiol* **14**: 1224–1239.

Ryu T, Seridi L, Moitinho-Silva L, Oates M, Liew YJ, Mavromatis C *et al.* (2016). Hologenome analysis of two marine sponges with different microbiomes. *BMC Genomics* **17**: 158.

Schläppy ML, Weber M, Mendola D, Hoffmann F, de Beer D. (2010). Heterogeneous oxygenation resulting from active and passive flow in two Mediterranean sponges, *Dysida avara* and *Chondrosia reniformis*. *Limnol Oceanogr* **55**: 1289–1300.

Schmitt S, Angermeier H, Schiller R, Lindquist N, Hentschel U. (2008). Molecular microbial diversity survey of sponge reproductive stages and mechanistic insights into vertical transmission of microbial symbionts. *Appl Environ Microbiol* **74**: 7694–7708.

Schmitt S, Tsai P, Bell J, Fromont J, Ilan M, Lindquist N *et al.* (2012). Assessing the complex sponge microbiota: core, variable and species-specific bacterial communities in marine sponges. *ISME J* **6**: 564–576.

Shaibe E, Metzer E, Halpern YS. (1985). Metabolic pathway for the utilization of L-arginine, L-ornithine, agmatine, and putrescine as nitrogen sources in *Escherichia coli* K-12. *J Bacteriol* **163**: 933–937.

Shimizu S, Kim J, Shinmen Y, Yamada H. (1986). Evaluation of two alternative metabolic pathways for creatinine degradation in microorganisms. *Arch Microbiol* **145**: 322–328.

Siegl A, Kamke J, Hochmuth T, Piel J, Richter M, Liang C *et al.* (2011). Single-cell genomics reveals the lifestyle of Poribacteria, a candidate phylum symbiotically associated with marine sponges. *ISME J* **5**: 61–70.

Solomon C, Collier J, Berg G, Glibert P. (2010). Role of urea in microbial metabolism in aquatic systems: a biochemical and molecular review. *Aquatic Microbial Ecol* **59**: 67–88.

Sona S, Suzuki T, Ellington WR. (2004). Cloning and expression of mitochondrial and protoflagellar creatine kinases from a marine sponge: implications for the origin of intracellular energy transport systems. *Biochem Biophys Res Commun* **317**: 1207–1214.

Spang A, Poehlein A, Offre P, Zumbragel S, Haider S, Rychlik N *et al.* (2012). The genome of the ammonia-oxidizing *Candidatus* Nitrososphaera gargensis: insights into metabolic versatility and environmental adaptations. *Environ Microbiol* **14**: 3122–3145.

Spieck E, Ehrich S, Aamand J, Bock E. (1998). Isolation and immunocytochemical location of the nitrite-oxidizing system in nitrospira moscoviensis. *Arch Microbiol* **169**: 225–230.

Spieck E, Bock E. (2005). The lithoautotrophic nitrite-oxidizing bacteriaIn:Brenner DJ, Krieg NR, Staley JT, Garrity GM, Boone DR, Vos PD *et al.* (eds). *Bergey's Manual of Systematic Bacteriology*. Springer Science +Business Media: New York, USA, pp 149–153.

Starkenburg SR, Chain PS, Sayavedra-Soto LA, Hauser L, Land ML, Larimer FW *et al.* (2006). Genome sequence of the chemolithoautotrophic nitrite-oxidizing bacterium *Nitrobacter winogradskyi* Nb-255. *Appl Environ Microbiol* **72**: 2050–2063.

Stieglmeier M, Alves RJE, Schleper C. (2014a). The Phylum ThaumarchaeotaIn:Rosenberg E, DeLong EF, Lory S, Stackebrandt E, Thompson F(eds). *The Prokaryotes: Other Major Lineages of Bacteria and the Archaea*4th edn.Springer-Verlag: Berlin, Heidelberg, Germany.

Stieglmeier M, Klingl A, Alves RJ, Rittmann SK, Melcher M, Leisch N *et al.* (2014b). *Nitrososphaera viennensis* gen. nov., sp. nov., an aerobic and mesophilic, ammonia-oxidizing archaeon from soil and a member of the archaeal phylum Thaumarchaeota. *Int J Syst Evol Microbiol* **64**: 2738–2752.

Su J, Jin L, Jiang Q, Sun W, Zhang F, Li Z. (2013). Phylogenetically diverse ureC genes and their expression suggest the urea utilization by bacterial symbionts in marine sponge *Xestospongia testudinaria*. *PLoS ONE* **8**: e64848.

Swem LR, Elsen S, Bird TH, Swem DL, Koch HG, Myllykallio H *et al.* (2001). The RegB/RegA two-component regulatory system controls synthesis of photosynthesis and respiratory electron transfer components in Rhodobacter capsulatus. *J Mol Biol* **309**: 121–138.

Tate Jr DJ, Miceli MV, Newsome DA. (1995). Phagocytosis and H2O2 induce catalase and metallothionein gene expression in human retinal pigment epithelial cells. *Invest Ophthalmol Vis Sci* **36**: 1271–1279.

Taylor MW, Schupp PJ, Dahllof I, Kjelleberg S, Steinberg PD. (2004). Host specificity in marine sponge-associated bacteria, and potential implications for marine microbial diversity. *Environ Microbiol* **6**: 121–130.

Taylor MW. (2005). *The ecology of marine sponge-associated bacteria* Ph.D. thesis The University of New South Wales: Sydney, Australia.

Taylor MW, Radax R, Steger D, Wagner M. (2007). Sponge-associated microorganisms: evolution, ecology, and biotechnological potential. *Microbiol Mol Biol Rev* **71**: 295–347.

Thomas T, Rusch D, DeMaere MZ, Yung PY, Lewis M, Halpern A *et al.* (2010). Functional genomic signatures of sponge bacteria reveal unique and shared features of symbiosis. *ISME J* **4**: 1557–1567.

Thomas T, Moitinho-Silva L, Lurgi M, Bjork JR, Easson C, Astudillo-Garcia C *et al.* (2016). Diversity, structure and convergent evolution of the global sponge microbiome. *Nat Commun* **7**: 11870.

van Kessel MA, Speth DR, Albertsen M, Nielsen PH, Op den Camp HJ, Kartal B *et al.* (2015). Complete nitrification by a single microorganism. *Nature* **528**: 555–559.

Wagner GP, Kin K, Lynch VJ. (2012). Measurement of mRNA abundance using RNA-seq data: RPKM measure is inconsistent among samples. *Theory Biosci* **131**: 281–285.

Walker CB, de la Torre JR, Klotz MG, Urakawa H, Pinel N, Arp DJ *et al.* (2010). Nitrosopumilus maritimus genome reveals unique mechanisms for nitrification and autotrophy in globally distributed marine crenarchaea. *Proc Natl Acad Sci USA* **107**: 8818–8823.

Webster NS, Thomas T. (2016). The sponge hologenome. *MBio* **7**: e00135-16.

Wetz MS, Wheeler PA. (2007). Release of dissolved organic matter by coastal diatoms. *Limnol Oceanogr* **52**: 798–807.

White D. (2007), The Physiology and Biochemistry of Prokaryotes. Oxford University Press: New York, NY, USA.

Willems A. (2014)The family Phyllobacteriaceae. In: Rosenberg E, DeLong EF, Lory S, Stackebrandt E, Thompson F(eds). *The Prokaryotes: Alphaproteobacteria and Betaproteobacteria*4th edn.Springer: Berlin, Germany, pp 355–418.

Wilson MC, Mori T, Ruckert C, Uria AR, Helf MJ, Takada K *et al.* (2014). An environmental bacterial taxon with a large and distinct metabolic repertoire. *Nature* **506**: 58–62.

Wulff J. (2012). Ecological interactions and the distribution, abundance, and diversity of sponges. *Adv Mar Biol* **61**: 273–344.

Wyss M, Kaddurah-Daouk R. (2000). Creatine and creatinine metabolism. *Physiol Rev* **80**: 1107–1213.

Yahel G, Sharp JH, Marie D, Hase C, Genin A. (2003). In situ feeding and element removal in the symbiont-bearing sponge *Theonella swinhoei*: bulk DOC is the major source for carbon. *Limnol Oceanogr* **48**: 141–149.

Zhalnina KV, Dias R, Leonard MT, Dorr de Quadros P, Camargo FA, Drew JC *et al.* (2014). Genome sequence of *Candidatus* Nitrososphaera evergladensis from group I.1b enriched from Everglades soil reveals novel genomic features of the ammonia-oxidizing archaea. *PLoS One* **9**: e101648.

Zheng H, Wisedchaisri G, Gonen T. (2013). Crystal structure of a nitrate/nitrite exchanger. *Nature* **497**: 647–651.

Supplementary Information accompanies this paper on The ISME Journal website (http://www.nature.com/ismej)